NEUROSCIENCE
RESEARCH ARTICLE
A. E. Morrissette et al. / Neuroscience 423 (2019) 55–65

Unilateral Optogenetic Inhibition and Excitation of Basal Ganglia Output Affect Directional Lick Choices and Movement Initiation in Mice

Arthur E. Morrissette,[a] Po-Han Chen,[a] Conrad Bhamani,[b] Peter Y. Borden,[c] Christian Waiblinger,[c] Garrett B. Stanley[c] and Dieter Jaeger[a]*

[a] *Department of Biology, Emory University, Atlanta, GA, United States*

[b] *Cornell University, Ithaca, NY, United States*

[c] *Department of Biomedical Engineering, Georgia Institute of Technology, Atlanta, GA, United States*

Abstract—Models of basal ganglia (BG) function predict that tonic inhibitory output to motor thalamus (MT) suppresses unwanted movements, and that a decrease in such activity leads to action selection. Further, for unilateral activity changes in the BG, a lateralized effect on contralateral movements can be expected due to ipsilateral thalamocortical connectivity. However, a direct test of these outcomes of thalamic inhibition has not been performed. To conduct such a direct test, we utilized rapid optogenetic activation and inactivation of the GABAergic output of the substantia nigra pars reticulata (SNr) to MT in male and female mice that were trained in a sensory cued left/right licking task. Directional licking tasks have previously been shown to depend on a thalamocortical feedback loop between ventromedial MT and antero-lateral premotor cortex. In confirmation of model predictions, we found that unilateral optogenetic inhibition of GABAergic output from the SNr, during ipsilaterally cued trials, biased decision making towards a contralateral lick without affecting motor performance. In contrast, optogenetic excitation of SNr terminals in MT resulted in an opposite bias towards the ipsilateral direction confirming a bidirectional effect of tonic nigral output on directional decision making. However, direct optogenetic excitation of neurons in the SNr resulted in bilateral movement suppression, which is in agreement with previous results that show such suppression for nigral terminals in the superior colliculus (SC), which receives a bilateral projection from SNr. **© 2019 IBRO. Published by Elsevier Ltd. All rights reserved.**

Key words: decision making, motor thalamus, substantia nigra, channel rhodopsin, mouse, learning.

INTRODUCTION

The basal ganglia (BG) are thought to influence the control of movement by inhibiting and facilitating selected motor programs to accomplish and reinforce goal-directed behavior (Albin et al., 1989; DeLong, 1990). Our long-standing understanding of the BG's role in the control of movement suggests that the output nuclei of the BG provide tonic inhibition over motor areas of the thalamus and brainstem to suppress unwanted movements; pauses in the inhibitory output would therefore facilitate movement initiation (Deniau and Chevalier, 1985; Mink, 1996; Hikosaka, 2007). In support of this general BG functional model, optogenetic activation of the BG direct pathway has been found to be pro-kinetic, leading to a reduction in the inhibition of the substantia nigra pars reticulata (SNr) (Freeze et al., 2013), the primary BG output nucleus in the rodent, and disinhibition of downstream targets (Oldenburg and Sabatini, 2015). Additionally, pauses in SNr activity preceded initiation of orienting movements in rats performing an auditory-cued Go–Stop task (Schmidt et al., 2013). It remains unclear, however, how cortical planning activity and motor initiation is affected by output from the BG.

Recent studies have shown that in mice the anterolateral premotor area (ALM) contributes to the initiation of directional licking in delayed choice tasks (Guo et al., 2014a; Li et al., 2015; Chen et al., 2017). ALM expresses ramping activity in a feedback loop with the ventromedial thalamus (VM) during preparation of directional licking, and inhibition of either area reduces task performance to chance (Guo et al., 2017). The VM thalamus is a major part of the BG input receiving motor thalamus (BGMT), which also includes a portion of the ventral anterior and lateral nuclei (Kuramoto et al., 2011). The BG are thus well positioned to control this corticothalamic feedback loop through their strong inhibitory projection to MT from the substantia nigra reticulata (SNr) and the globus pallidus internus (GPi). Directional licking behavior as planned

*Correspondence to: Dieter Jaeger, Department of Biology, Emory University, 1510 Clifton Road NE, Atlanta, GA 30322, United States.
E-mail address: djaeger@emory.edu (D. Jaeger).
Abbreviations: BG, basal ganglia; MT, motor thalamus; SC, superior colliculus; SNr, substantia nigra pars reticulata; VM, ventromedial thalamus.

https://doi.org/10.1016/j.neuroscience.2019.10.031
0306-4522/© 2019 IBRO. Published by Elsevier Ltd. All rights reserved.

and initiated by ALM presents therefore an ideal model system to study how the BG exert motor effects in cortically initiated movements. To address this question, we trained mice to perform a licking task where they must lick a left or right positioned lick spout following a left or right air puff, respectively. Using optogenetic methods to inhibit SNr neurons unilaterally, we found that silencing the inhibitory output of the BG triggered licking contralateral to the side of inhibition, irrespective of the rewarded licking direction. In contrast, exciting SNr projections to the MT and inhibiting thalamic activity suppressed contralateral licking and biased licking towards ipsilateral direction. These results confirm that the BG output via SNr to the MT exerts powerful unilateral control over movement preparation and initiation in the context of sensory guided motor behavior. However, directly stimulating GABAergic neurons in SNr resulted in bilateral inhibition of licking during the stimulus period, suggesting a descending bilateral pathway, likely via superior colliculus (SC) (Rossi et al., 2016; Toda et al., 2017).

EXPERIMENTAL PROCEDURES

Animals

All experimental procedures were approved by the Emory University Institutional Animal Care and Use Committee. For optogenetic stimulation and electrophysiological experiments, male and female Vgat-IRES-Cre mice (*Slc32a1*) aged 6–12 months at the start of experiments were used. Mice were maintained on a 12 h:12 h reverse light cycle and all experiments and behavioral training was performed during the dark portion of the cycle. Mice undergoing behavioral training were provided *ad libitum* food access and were kept on 1–1.5 ml/day water restriction 6 days a week starting at least 3 days prior and for the duration of handling, training, and experimental testing. On day 7 of each week, mice were given free access to water. During behavioral training and testing, mice were given 10% sucrose solution with 0.1% grape Kool-Aid powder. Liquid consumption was measured during testing and mice were supplemented with water to reach the 1–1.5 ml/day volume. A total of 15 mice with successfully targeted AAV injections were used in the study. Eleven mice were used in behavioral experiments and four mice were used for electrophysiological recordings.

Surgery

Viral vector injection and fiber placement. For optogenetic AAV vector injection, mice were anesthetized with isoflurane (induction at 3–4%, maintained at 1–2%) and head-fixed on a stereotaxic frame (Kopf). Craniotomies were made unilaterally above the SNr. For somatic SNr inhibition, 200 nL of AAV5-EF1a-DIO-eARCH3.0-eYFP (ARCH; $n = 5$, 3 male) or for excitation, 200nL of AAV5-EF1a-DIO-hChR2(E123T/T159C-EYFP (ChR2(ET/TC) or ChR2; $n = 4$, 2 male) was injected with a nano-injector (Nanoject II, Drummond Scientific) at the rate of 0.46 nl/s into the SNr targeting the coordinates (in mm from Bregma): AP −3.2, ML 1.6, DV −4.2). For somatic SNr excitation and SNr-BGMT terminal excitation 200 μm, 0.22NA optic fibers (Thor Labs) each with a 1.25 mm steel ferrule were then implanted targeting the SNr and the VM (AP −1.5, ML 0.9, DV −4.0). Following surgical implantation, mice were kept in single housed cages. All optogenetic manipulations were performed unilaterally on the right side of the animal, and hence 'ipsilateral' (IPSI) in this paper always refers to the right and 'contralateral' (CONTRA) refers to the left side of the body.

Acute electrode/optrode recordings. To record and/or optogenetically manipulate neural populations in the right SNr or downstream projection targets, a craniotomy was made above the site targeting these areas and the dura was kept intact. A 4 mm diameter and 1 mm tall plastic tube was glued in place around the craniotomy and the area was filled with a removable elastomer (Kwik-Cast, World Precision Instruments) to allow for access to the tissue for future experiments.

Behavior

Prior to behavioral training, a custom stainless-steel head-post was attached posterior to lambda by placing a thin layer of cyanoacrylate adhesive on the skull, followed by a thin layer of dental acrylic (Metabond; C&B Associates). Following recovery, mice were head-fixed and placed within the behavioral training setup consisting of two 2 mm diameter lick spouts placed 5 mm apart and two 2 mm diameter air-puff tubes that were directed at the C row of whiskers. The lick spouts were connected to a custom capacitive lick sensor circuit that recorded time and duration of licks at 200 Hz. Air-puff intensities were calibrated such that whisker deflection was apparent under high-speed video monitoring without signs of freezing or startle behavior from the mouse.

Behavioral task

Animal training protocols and behavioral paradigm are adapted from previously reported procedures (Guo et al., 2014b). The behavioral paradigm is illustrated in Fig. 1A. Left and right air-puff/lick trials were selected pseudo-randomly such that the probability of a left/right trial was adjusted based on the ratio of left/right rewarded trials for a given session:

$$P_L(i) = \frac{\sum_1^i C_R(i)}{\sum_1^i C_L(i) + \sum_1^i C_R(i)}$$

where C_X(i) is 1 or 0 for trial i in the x direction for a correct or incorrect trial, respectively. This procedure leads to an equal number of left/right trials when the probability of success is equal, but will increase the number of trials towards a lick direction in which a mouse showed increased fail probability during a given session. This enforcement of licking towards an 'unpopular' direction was needed because mice tend to perform repetitive behaviors towards one direction when this behavior only occasionally has negative consequences (no reward). It presented an effective way to train mice to attend to both lick spouts equally in baseline behavior.

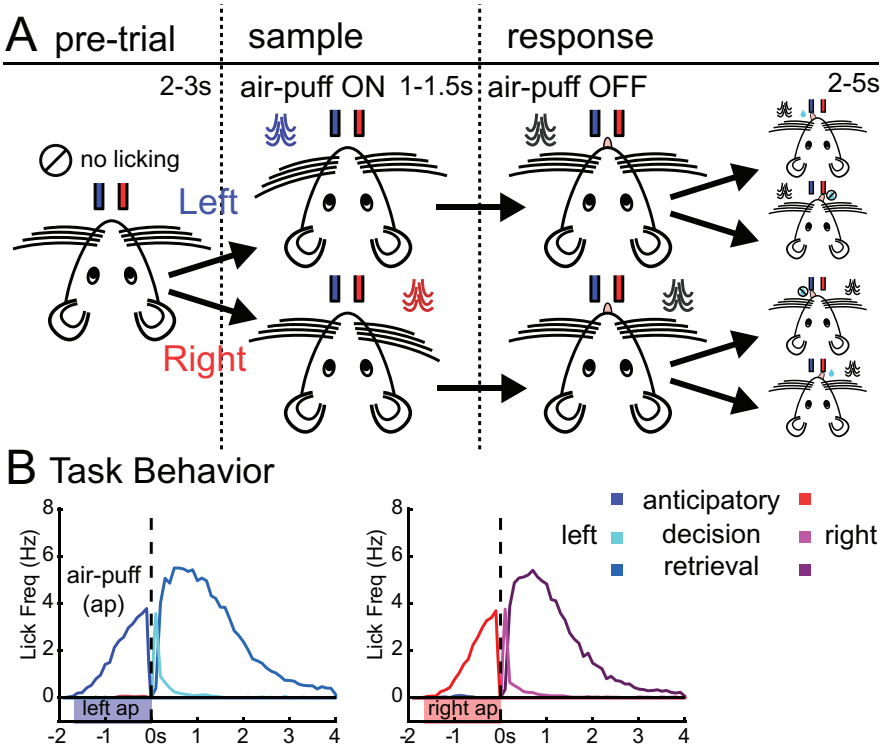

Fig. 1. Learning of forced choice licking task. (A) Illustration of the forced choice licking task. Each trial begins with a pre-trial period lasting 2–3 s where the mouse must not lick either spout. During the sample period, an air-puff is directed at either the left or right whiskers and remains on for 1–1.5 s. The response period begins after the offset of the air-puff and the first lick during this period is counted as the decision lick. If the decision lick is correct (towards the left spout for left air-puff or right lick spout for right air-puff) the mouse is provided a liquid reward from the correct spout. If the mouse does not provide a lick for the duration of the response period (2–5 s) or licks the incorrect spout no reward is provided. (B) Average lick frequency traces for correct trials from mice performing the anticipatory variant of the task (n = 12 mice). Left. For left trials (n = 1151 trials), Mice begin to show anticipatory licking (middle blue) after the onset of the air-puff and the first lick after the offset of the air-puff is counted as the decision lick (light blue). The retrieval licks (dark blue) are the licks corresponding to the mouse retrieving the sucrose reward after a correct decision lick. Right. Same format as left trials, but instead showing right trials (n = 1098). Anticipatory, decision, and retrieval licks are depicted as middle red, light red, and dark red, respectively.

Each trial was made up of 3 discrete intervals: a ‘‘pre-stimulus” period, a ‘‘sample” period where mice received either a left or right air-puff for 1–1.5 s, followed by a 5 s ‘‘response” period where the mice lick the left or right spout to indicate which spout they believe will be rewarded and then consume the reward if the correct choice was made. Trials were separated by a variable inter-trial period. During the sample period, mild non-aversive air-puff stimuli were directed through 2 mm-diameter steel tubes towards the whiskers. The tubes were angled at 15 degrees away from the mouse center to isolate air-puff stimuli to the whiskers, avoiding the face of the mouse. The stimuli lasted for 1–1.5 s.

Training for the behavioral task began after a minimum of 10 days following surgery and 5 days following the start of water restriction. Mice were handled during initial days of water restriction to acclimate with handling. On the first day of head-fixation and training, mice were secured in the holder and placed in the behavioral setup with the two lick spouts positioned and centered in front of the mouth of the mouse. During the first day of training, mice could lick both the left or right spout and would receive a sucrose reward following licks at a minimum interval of 10 s. This was primarily used to acclimate the mouse with head-fixation and the positions of the lick spouts. The positions of the spouts were manually adjusted relative to the center of the mouth to promote equal licking of both lick spouts. During subsequent days of training, mice were transitioned to a task where the air-puffs signifying the rewarded spout were active, though the reward was automatically triggered (‘‘Auto-Reward”). This typically lasted 1 day of training (∼4 50 trial blocks) until the mice became acclimated to the puffs and would display anticipatory licking towards the correct lick spout before the reward was triggered, demonstrating that the mice had built the association between air-puff location and rewarded lick spout. In the next step of training, typically occurring on days 2–3, mice received the air-puffs and were then allowed to lick freely towards both spouts in the Response period and were only rewarded on licks to the correct spout (‘‘Free-Lick”). Mice during this time learned to make the correct perceptive decision (signified by licking the rewarded spout exclusively during trials). To minimize licking outside of the response interval of the trials, each trial began with a pre-stimulus period where the mouse was required to withhold licking for at least 2–3 s before air-puff onset. Licking during the last second of this period led to a trial fail and mice were placed back in the inter-trial period awaiting the start of the next trial. During the subsequent stimulus period mice were allowed to perform ‘anticipatory’ licks, however, where they could touch either lick tube. A total of 12 mice were trained.

Optogenetic stimulation

Before and after each session the output intensity of the light source (either LED or laser) was determined using an optical power meter and sensor (PM100D and S121C, ThorLabs). For SNr inhibition experiments, we used a 593 nm yellow laser (Shanghai Dream Lasers) collimated and coupled to a 200 μm, 0.22 NA patch cable (Doric Lenses) leading to 8–12 mW output from the fiber tip. For somatic SNr excitation we used a 470 nm LED (Doric Lenses) coupled to the same patch cable with output power between 1 and 3 mW from fiber tip. Finally, for SNr-BGMT terminal excitation, we used a

470 nm blue laser (Shanghai Dream Lasers) with the same patch cables with output power between 8 and 12 mW from the fiber tip. Trials with optogenetic stimulation were randomly intermixed with control trials for a total proportion of 50% for ARCH stimulation and only 25% for ChR2 stimulation due to a concern that optical ChR2 stimulation effects may negatively impact baseline behavior. The optical stimulation trials were also all executed with a fixed 1 s air-puff duration in order to avoid inconsistent relations between stimulation and the timing of anticipatory licking. All optogenetic stimuli were set to a duration of 1 s and were centered on the offset of the air-puff. Optogenetic stimuli were aborted as soon as the mouse executed a decision lick and a trial transitioned from the response period to either reward period (correct lick direction), or the failure period (wrong lick direction).

Electrophysiology

During surgical preparation, a craniotomy was made over the future right SNr/BGMT recording sites (−4 to 1 mm AP, 0.5–2.5 mm ML) and covered with Kwik-cast (WPI Inc.). The dura was left intact. A stainless-steel reference skull screw (#19010-10, Fine Science Tools) was placed over the contralateral sensory cortex. A 0.01″ diameter steel wire was soldered between the screw and a gold pin to connect to the acquisition system during recording. The mice were allowed at least 3 days to recover. Following recovery, mice were acclimated to being head-fixed and recording sessions began (one session per day, 2 h per session). Within the first session of head-fixation, mice showed no overt signs of stress and appeared relaxed. During recording, mice were maintained on a randomized interval reward paradigm where mice were provided with a sucrose reward via right or left lick spout every 30–60 s to encourage quiet wakefulness during the session. At the start of the session, the Kwik-cast cover over the craniotomy was removed. Custom optrodes consisting of a 50–100 μm optic fiber (ThorLabs) attached 200–300 μm above a micro-electrode (FHC) were lowered into the SNr or BGMT. Raw signals (0.1–10 kHz band-pass filtered) were acquired at 20 kHz, amplified and digitized (RHD2132 headstage, Intan Technologies) and saved (RHD2000 Evaluation System/Interface Software, Intan Technologies). Once unit activity was detected in the SNr or BGMT, optical stimulation with either a yellow (593 nm) or blue (473 nm) laser was delivered for 1 or 2 s continuous pulses every 10 s to stimulate ARCH3 or ChR2 expressing neurons, respectively. For some recordings, the optic fiber was placed in the SNr with a separate electrode lowered in to the BGMT for recording activity downstream of the site of optogenetic stimulation. After each session, the craniotomy was covered with Kwik-cast and following the final recording session, the mouse was perfused with PBS followed by perfusion with 4% paraformaldehyde and 15% sucrose. The brain was then removed and transferred to a 4% paraformaldehyde/30% sucrose solution for later histological processing.

Data analysis

Analysis of behavioral and electrophysiological data was performed in MATLAB (MathWorks). Only behavioral sessions where baseline performance was above 60% were included in analysis. Behavioral trials in which the mouse licked < 1 s before the start of the trial (onset of the air-puff) were caught and sent to inter-trial delay. These trials were rare (< 2% in trained mice and excluded from analysis). Lick data were pre-processed to remove "artifact licks" (spout contacts shorter than 10 ms and contacts lasting longer than 200 ms typically caused by electrical noise and paw touches, respectively). Trials where the decision lick (first lick during the response period) was classified as an artifact lick were removed from subsequent analyses. To calculate average lick frequencies for the various behavioral and experimental conditions, the onsets of lick contacts were marked and lick contacts across each trial were summed in 50 ms bins and divided by the length of the bin duration. Hierarchical bootstrapping provides an unbiased method by which multi-level samples can be analyzed for significant outcomes while accounting for intra- and interlevel sample correlations (Efron and Tibshirani, 1993; van der Leeden et al., 2008; Aarts et al., 2014). We followed the procedure used by Guo et al. (2014a) to determine the significance of the performance change in each optogenetic stimulation condition using bootstrapping to account for variability across mice, sessions, and trials. We tested against the null hypothesis that the performance change seen with optogenetic stimulation was due to normal behavioral variability. In each round of bootstrapping, we replaced the original data set with a re-sampled set in which we resampled with replacement from: (1) animals; (2) sessions performed by each animal; and (3) the trials within each session with the number of trials in a given session preserved. We then computed the change in performance on the re-sampled data set. Repeating this procedure 10,000 times produced a distribution of performance changes that reflected the behavioral variability. The P value observed performance change was calculated as the fraction of times bootstrapping produced an inconsistent performance change (for example, if a performance decrease was observed during optogenetic stimulation, the P value is the fraction of times a performance increase was observed during bootstrapping, one-tailed test). Error bars represent the +/− SEM generated from bootstrapping unless noted otherwise.

RESULTS

Mouse behavioral performance in bidirectional forced choice licking task

In order to understand how the BG output influences movement initiation and decision making, we employed a forced choice left/right lick task (See Methods, Fig. 1A). After training was complete, mice correctly discerned which side whiskers were stimulated at with a mild air-puff, and frequently started licking on the correct side in anticipation of the reward while the air-puff was

still being delivered (Fig. 1B). However, only the first lick after the air-puff turned off was used to determine if the correct side was touched, and was therefore defined as the 'decision lick'. A decision lick on the correct side lead to immediate reward delivery, and subsequent consummatory 'retrieval licking' by the mice.

Unilateral inactivation of the SNr biases towards contralateral licking behavior

We began assessing the role of BG output in performing the forced choice licking task, using fast, reversible optogenetic inactivation of the SNr through nigral ARCH3 activation (Fig. 2A). Cre-dependent ARCH3 was injected to the SNr of VGAT-cre mice that express cre in GABAergic populations. Extent of expression was well localized to the SNr with axon terminals extending towards known projection targets of the SNr such as the substantia nigra compacta, brainstem and thalamus (typical example shown in Fig. 2A). In awake mice at rest, yellow (593 nm) light stimulation of SNr neurons expressing ARCH3 abolished nearly all firing activity for the duration of the stimulation (mean firing rates 17.2 Hz baseline vs. 2.61 Hz with ARCH inhibition, $n = 10$ single units, Fig. 2B, C). Following the offset of the optogenetic stimulation, the firing rate quickly returned to baseline levels. In behaving mice, we optogenetically manipulated the SNr unilaterally in the right hemisphere (Fig. 2D). To examine the role of the SNr in anticipatory licking activity, the SNr was inhibited from 0.5 s before the offset of the air-puff until 0.5 s into the response period of the task. Inhibiting the right SNr during this period biased licking activity towards the contralateral direction (Fig. 2E, H1, H2, 5 mice, 36 sessions). A striking increase in error trials with ipsilateral air-puff but contralateral decision licks was observed (Fig. 2H2, $P < 0.001$, bootstrap) and the overall success rate of ipsilateral trials was decreased (Fig. 2H1, $P < 0.001$, bootstrap). In addition, the contralateral bias was expressed by an increase in successful trial performance with contralateral air-puffs (Fig. 2H1, $P < 0.001$, bootstrap), which was due to a decrease in contralateral no-response trials (Fig. 2H3, $P < 0.001$, bootstrap). Importantly, successful trials showed the same amount and timing of anticipatory licking and the same consummatory lick rate in trials with air-puffs on either side with or without SNr inhibition (Fig. 2F1-2). This suggests that the lateralization of decision making towards the spout contralateral to SNr inhibition was not due to a slowing of movement, but rather a categorical change in the decision process. In control mice expressing an EYFP virus without ARCH3, light stimulation had no effect on licking behavior or task performance (2 mice, 11 sessions, Fig. 2IJ1-J3).

Unilateral excitation of the SNr impairs both contra- and ipsilateral licking activity

Since inhibiting BG output resulted in a contralateral bias in movement initiation and preparation, the classic model of BG rate coding leads to the prediction that increasing BG output would exert an opposite effect on licking activity, namely a reduction of correct decisions to lick in the direction contralateral to optogenetic stimulation. To test this prediction, we used the neural activator, ChR2 (ET/TC), to increase output activity from the SNr (Fig. 3A). The extent of the ChR2(ET/TC) opsin expression was again well localized to the SNr and SNr terminals observable in the VM thalamus and brainstem (typical example shown in Fig. 3A, right). In awake mice, blue light (473 nm) stimulation of the SNr using a 1 s continuous pulse increased the already highly active SNr to 3.6 times the baseline firing rate for the duration of the light stimulation (mean firing rate at baseline = 13.9 Hz vs. opto = 49.9 Hz, $n = 8$ single units, Fig. 3B, C). In mice performing the forced choice licking task ($n = 4$ mice, 16 sessions, Fig. 3D–F), exciting the right SNr almost completely suppressed both contralateral and ipsilateral licking activity for the duration of the optogenetic stimulation after anticipatory licking had already started in the first 0.5 s of the air-puff (Fig. 3E, F1-2, in F1 anticipatory lick suppression is shown by the difference between black and blue (F2: red) lines before air-puff offset at time 0, and decision lick suppression is shown by difference between light grey and cyan (F2: purple) traces following air-puff offset.). Following the offset of the optogenetic perturbation, mice often resumed licking towards the correct spout (Fig. 3E, F1-2, H1, H2, in F1 note a peak in the cyan (F2: purple) trace after laser stimulation offset indicating a rebound in correct decision lick activity). However, over all mice and sessions there was a significant increase of licking the wrong spout direction (Fig. 3H2, $P < 0.01$ (contralateral trials), $P < 0.001$ (ipsilateral trials), bootstrap), suggesting a partial loss of the neural representation of lick direction during the nigral excitation. An increased percentage of trials with failure to lick during the response period was also observed (Fig. 3H3), which due to high inter-session and inter-mouse variability was not significant on the contralateral side and only reached marginal significance ipsilaterally (Fig. 3H3, $P < 0.05$ (ipsilateral trials), bootstrap). In combination these errors lead to a significant decrease in both contralateral and ipsilateral task performance with ChR2 stimulation (Fig. 3H1, $P < 0.01$, bootstrap). In control mice injected with an EYFP virus without ChR2, blue light stimulation had no effect on licking behavior or task performance ($n = 2$, Fig. 3I, J). These results give a more complex picture of bidirectional motor control with SNr inhibition or excitation than predicted by the classic rate model (Albin et al., 1989; Alexander et al., 1990). Particularly striking was a complete bilateral lick cessation during ChR2 induced SNr rate increases, which was distinctly different from the lateralized effects of ARCH inhibition.

Unilateral excitation of nigrothalamic terminals in BGMT primarily impedes licking towards the contralateral direction in the anticipatory task variant

The differences in effects described for somatic SNr inhibition and excitation may be due to descending projections from the SNr towards the brainstem as well as ascending projections to BGMT. To begin to resolve

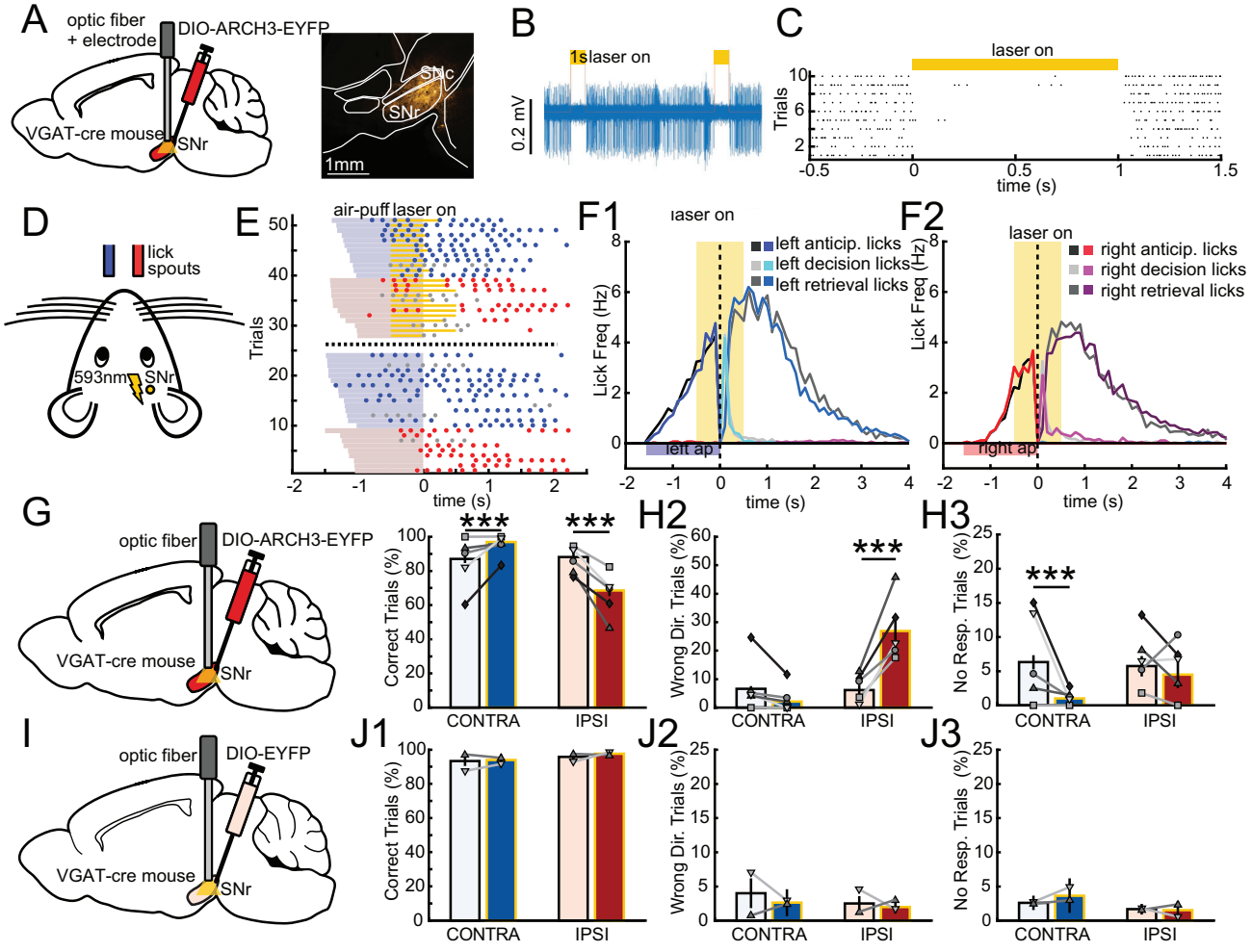

Fig. 2. Unilateral inactivation of the SNr biases towards contralateral licking behavior. (A) Diagram of optogenetic vector injection and optic fiber targeting. Cre-dependent AAV2-DIO-ARCH3-EYFP was injected in the right SNr of VGAT-cre transgenic mice and optic fiber attached to a microelectrode was lowered into SNr. Example of ARCH3-EYFP (yellow) expression in SNr (right). Photos were taken of EYFP fluorescence in fixed 50 μm coronal slices, and false yellow color was applied. The anatomy overlay is taken from the Allen mouse brain atlas. (B) Example single-unit recording of an SNr neuron expressing ARCH3. 593 nm laser stimulation silences firing activity for the duration of the light pulse and firing quickly resumes following the offset of the light stimulation. (C) 10 stimulation trials aligned to the onset of stimulation that show the consistency of ARCH3 inhibition of SNr activity. (D) Illustration showing mouse orientation with respect to ipsilateral (red) and contralateral (blue) lick spouts positioned in front of the mouse and optogenetic illumination through fiber implanted over the SNr. (E) Example behavioral session showing licking activity for ipsilateral and contralateral optogenetic and baseline trials. Trials are arranged by optogenetic stimulation condition (stim trials top, baseline below) and length of air-puff presentation. Blue and red horizontal lines depict the presentation of the air-puff during the sample period and yellow lines are the periods of optogenetic SNr inhibition. Blue dots denote contralateral licks with contralateral cues, red dots denote ipsilateral licks with ipsilateral stimulation, and gray dots denote licks to the incorrect side. In this example, optogenetic inhibition of right SNr disrupts right (ipsilateral) licking behavior such that the mouse is biased towards licking the contralateral spout, hence an increase in gray dots for ipsilateral trials. (F) Average lick frequency traces for correct trials with (colored lines) and without (gray lines) optogenetic SNr inhibition. For contralateral trials (n = 300 opto, 247 baseline, F1) and ipsilateral trials (n = 185 opto, 301 baseline, F2) mice show anticipatory licking activity towards the correct spout that increases until the start of the response period. Anticipatory licks are depicted by the middle colored line, followed by decision licks (light color) and retrieval licks (dark colored line). (G) Behavioral effects of unilateral SNr optogenetic inhibition in the anticipatory task. (H) Changes in performance between contralateral (blue) and ipsilateral (red), off (light) and on (dark) stimulation. Bar height represents mean across all sessions (n = 35 sessions), with shapes representing the mean for each mouse (5 mice). Error bars represent SEM (bootstrap, 10,000 iterations) and p values based on bootstrap (see methods, ***P < 0.001, **P < 0.01, *P < 0.05). (H1) B Compared to interleaved baseline trials (light blue/red columns), licking performance during unilateral SNr inhibition (dark blue/red columns) produced a significant increase in the percent of contralateral trials correct (P < 0.001) and significant decrease in the percent of ipsilateral trials correct (35 sessions, 5 mice). (H2) Optogenetic inhibition of the SNr caused a significant increase (P < 0.001) in the percent of ipsilateral wrong direction fail trials (incorrectly lick contralateral spout during ipsilateral trials). (H3) For contralateral lick trials, SNr inhibition significantly reduced the number of no response trials (P < 0.001). (I) Behavioral effects of yellow light stimulation in two control mice expressing EYFP in the anticipatory task. (J) No significant changes in performance were observed between contralateral and ipsilateral trials, off and on stimulation for percentage correct trials (J1), wrong direction trials (J2), or no response trials (J3).

the functional differences between these projection pathways, we selectively targeted the ascending pathway from the SNr to the BGMT. To achieve this, we stimulated ChR2 expressing SNr terminals in BGMT in the same mice used for somatic stimulation through a second fiber implanted over the BGMT. In contrast to

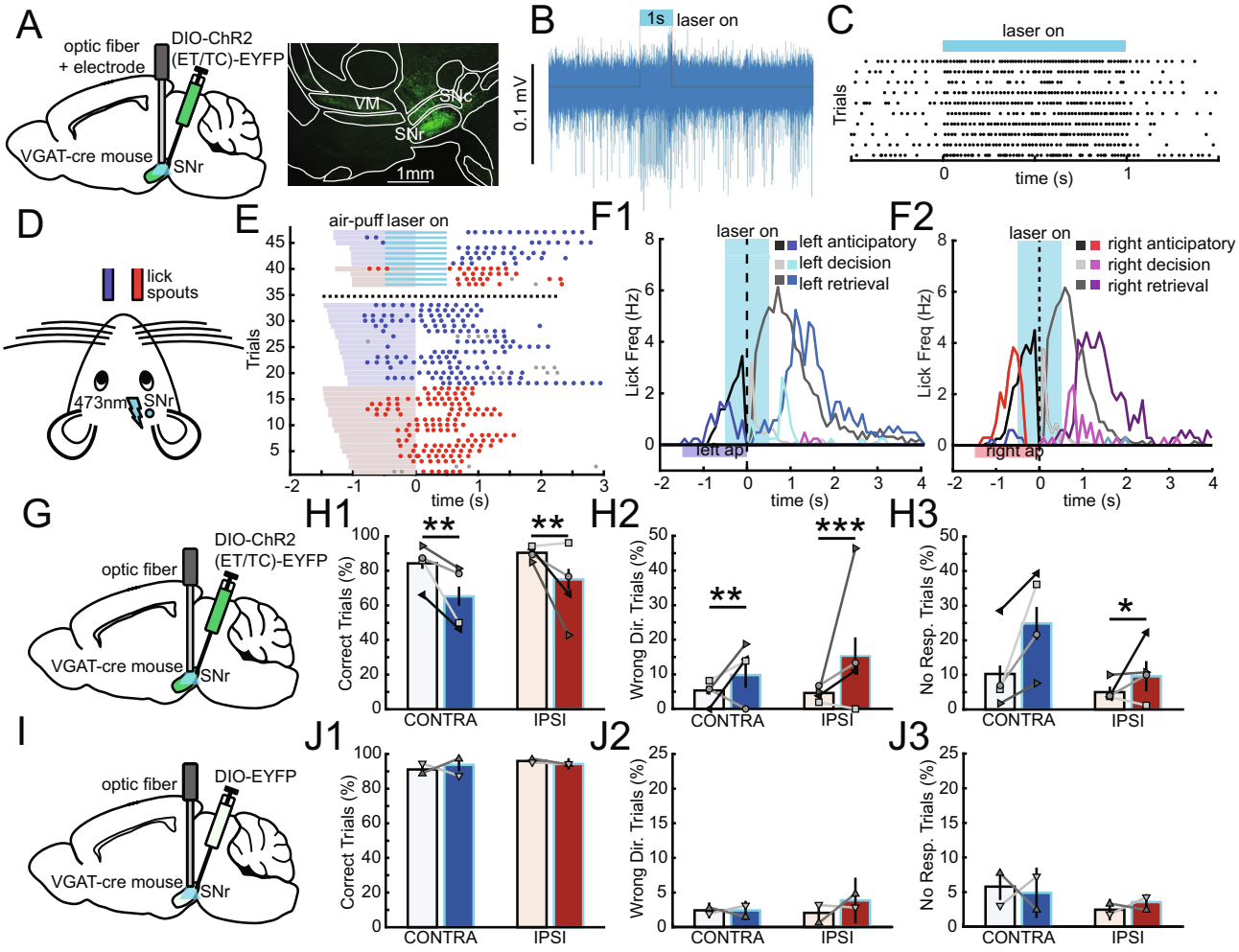

Fig. 3. Unilateral excitation of the SNr impairs both contra- and ipsilateral licking activity. (A) (left) Diagram of optogenetic vector injection and optic fiber targeting. Cre-dependent AAV2-DIO-hChR2(E123T/T159C)-EYFP was injected in the right SNr of VGAT-cre transgenic mice and optic fiber attached to a microelectrode was lowered in to SNr. (right) Example of ChR2(ET/TC)-EYFP expression (green) in SNr and axonal projections in VM thalamus and brainstem areas. Photos were taken of EYFP fluorescence in fixed 50 μm coronal slices, and false green color was applied. The anatomy overlay is taken from the Allen mouse brain atlas. (B) Example multi-unit recording of an SNr neuron expressing ChR2(ET/TC). 473 nm laser stimulation increases firing activity for the duration of the light pulse and firing quickly resumes following the offset of the light stimulation. (C) 10 stimulation trials aligned to the onset of stimulation that show the excitation of SNr activity across trials (single unit isolated from recording shown in (B). During ChR2 excitation, mean firing rate increased from 13.9 Hz to 49.9 Hz (n = 10 neurons). Firing rate increase of example neuron is 14.4 Hz vs. 46.3 Hz during optogenetic stimulation. (D) Illustration showing mouse orientation with respect to right and left lick spouts positioned in front of the mouse and optogenetic illumination through fiber implanted over the SNr. (E) Example behavioral session showing licking activity for ipsilateral and contralateral optogenetic and baseline trials. Annotation as in Fig. 2E. In this example, optogenetic excitation of SNr disrupts licking behavior both ipsilateral and contralateral to the side of optogenetic stimulation, though licking resumes following the offset of the light. Note that a single behavioral session of one mouse does not represent the overall lick statistics, which are shown in traces in panel (F). (F). Average lick frequency traces for correct trials with (colored lines) and without (gray lines) optogenetic SNr excitation across sessions and mice. For contralateral trials (n = 96 opto, 168 baseline, F1) and ipsilateral trials (n = 103 opto, 153 baseline, F2) mice show anticipatory licking activity towards the correct spout that increases until the start of the response period for baseline licking, though is suppressed following the onset of light stimulation for optogenetic trials. Anticipatory licks are depicted by the middle colored line, followed by decision licks (light color) and retrieval licks (darkest color). (G) Behavioral effects of unilateral SNr optogenetic excitation in the anticipatory task. (H) Changes in performance between contralateral (blue) and ipsilateral (red), off (light) and on (dark) stimulation. Bar height represents mean across all sessions (n = 16 sessions), with shapes representing the mean for each mouse (4 mice). Error bars represent SEM (bootstrap, 10,000 iterations) and p values based on bootstrap (see methods, ***p < 0.001, **p < 0.01, *p < 0.05). (H1) Compared to baseline trials (light blue/red columns), licking performance during right SNr excitation (dark blue/red columns) produced a significant decrease in the percent of contralateral and ipsilateral trials correct (p < 0.01, 16 sessions, 4 mice). (H2) Optogenetic excitation of the SNr caused a significant increase in the percent of wrong direction fail trials for both contralateral (P < 0.01) and ipsilateral (P < 0.001) trials. (H3) For contralateral lick trials, SNr excitation showed a trend towards increase percentage of no response trials (P = 0.094) and a marginally significant increase in no response trial percentage for ipsilateral lick trials (P < 0.014). (I) Behavioral effects of blue light stimulation in control mice expressing EYFP in the anticipatory task. (J) No significant changes in performance were observed between contralateral and ipsilateral trials, off and on stimulation for percentage correct trials (J1), wrong direction trials (J2), or no response trials (J3).

somatic stimulation we found that SNr terminal stimulation in BGMT in the anticipatory variant of the task suppressed only contralateral licking behavior and did not affect ipsilateral (right) lick activity (4 mice, 25 sessions, Fig. 4B, C, in panel 4C1 note left lick suppression during laser stimulation similar to Fig. 3F1,

but in panel 4C2 there is no such right lick suppression compared to panel 3F2). Nevetheless, ipsilateral trials did show a small increase of wrong direction lick trials (Fig. 4E2, $P = 0.02$, bootstrap). While this ipsilateral failure increase was marginally significant, it was not associated with a significant decrease in correct trials (Fig. 4E1), and we tend to think this may be a spurious outcome based on the very small number of trials involved (less than 2% of the total trials). Successful trial execution was significantly impaired for contralateral lick trials but remained unchanged for ipsilateral licks (Fig. 4E1, $P < 0.001$ (contralateral), bootstrap). This change in performance was due to an increase of contralateral air-puff failed trials both by not responding (Fig. 4E3, $P < 0.001$, bootstrap) as well as licking in the wrong direction (Fig. 4E2, $P < 0.001$, bootstrap). Terminal excitation in mice expressing EYFP without ChR2 did not demonstrate any changes in licking performance ($n = 2$, Fig. 4F, G).

DISCUSSION

Our results demonstrate that optogenetic inhibition of BG output from the SNr in mice strongly influences the control of directional licking. Specifically, unilateral inhibition of the SNr with ARCH activation leads to a biasing in licking towards the contralateral side (Fig. 2). In contrast, unilateral excitation of SNr with ChR2 resulted in a pronounced decrease of licking towards both sides. However, direct excitation of SNr terminals in BGMT thalamus with ChR2 affected predominantly contralateral trials, leading to an increase in wrong direction decisions and failures to respond (Figs. 4 and 5). These findings overall indicate that the unilateral SNr firing rate

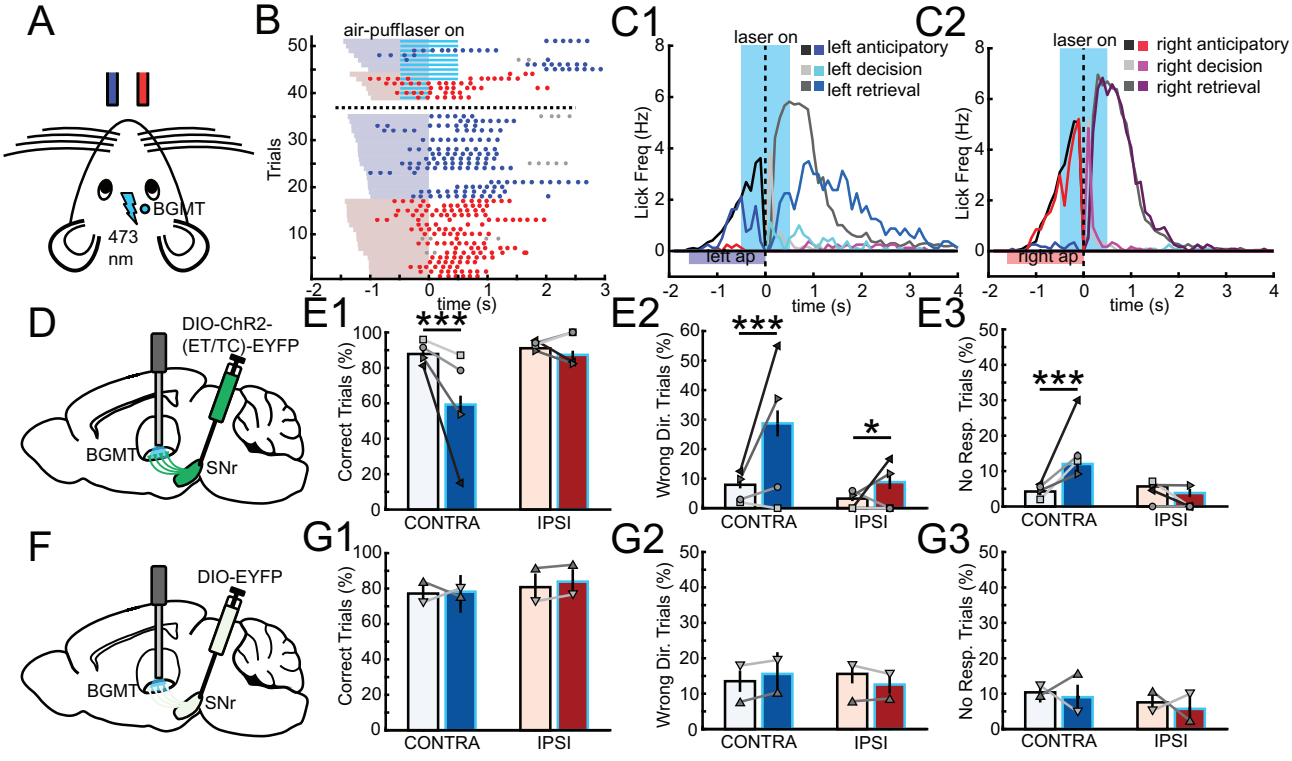

Fig. 4. Unilateral excitation of SNr projections to the BGMT primarily impairs licking towards the contralateral direction. (A) Diagram showing mouse orientation with respect to right and left lick spouts positioned in front of the mouse and optogenetic illumination through fiber implanted over the BGMT. (B) Example behavioral session showing licking activity for ipsilateral and contralateral optogenetic and baseline trials during the anticipatory task. Annotation as in Fig. 2E. In this example, optogenetic excitation of right SNr-BGMT projections disrupts only contralateral licking behavior during optogenetic stimulation trials. (C) Average lick frequency traces for correct trials with (colored lines) and without (gray lines) optogenetic right SNr-BGMT terminal excitation. For contralateral trials ($n = 95$ opto, 310 baseline, C1) and ipsilateral trials ($n = 128$ opto, 297 baseline, C2) mice show anticipatory licking activity towards the correct spout that increases until the start of the response period for baseline licking, though anticipatory licking is suppressed following the onset of light stimulation for contralateral optogenetic trials. Anticipatory licks are depicted by the middle colored line, followed by decision licks (light color) and retrieval licks (dark color). (D) Behavioral effects of unilateral SNr-BGMT optogenetic excitation in the anticipatory task. € Changes in performance between contralateral (blue) and ipsilateral (red), off (light) and on (dark) stimulation. Bar height represents mean across all sessions ($n = 25$ sessions), with shapes representing the mean for each mouse (4 mice). Error bars represent SEM (bootstrap, 10,000 iterations) and p values based on bootstrap (see methods, ***$p < 0.001$). (E1) Compared to baseline trials (light blue/red columns), licking performance during right SNr-BGMT terminal excitation (dark blue/red columns) produced a significant decrease in the percent of contralateral trials correct ($p < 0.001$, 25 sessions, 4 mice). (E2) Optogenetic excitation of the right SNr-BGMT terminals caused a significant increase in the percent of contralateral ($P < 0.001$) and ipsilateral ($P = 0.02$) wrong direction fail trials. (E3) For contralateral lick trials, SNr-BGMT terminal excitation caused a significant increase in the percentage of no response trials ($P < 0.001$). (F) Behavioral effects of blue light stimulation in control mice expressing EYFP in SNr terminals in BGMT in the anticipatory task. (G) No significant changes in performance were observed between contralateral and ipsilateral trials, off and on stimulation for correct trials (G1), wrong direction trials (G2), or no response trials (G3).

decreases are biasing lick direction choice, and that unilateral SNr rate increases suppress licking bilaterally. In mice performing a similar directional licking task, suppressing activity in either the VM thalamus, which is a major component of BGMT, or the ALM premotor cortex, through either optogenetic or muscimol inactivation selectively disrupts contralateral licking, while leaving ipsilateral licking unaffected (Li et al., 2015, 2016; Chen et al., 2017; Guo et al., 2017; Svoboda and Li, 2017). Our results therefore indicate that this thalamo-cortical motor planning process can be gated by BG output in agreement with traditional rate coding concepts of BG – cortical loops (Alexander et al., 1990). According to this model, inhibiting the SNr with ARCH unilaterally leads to disinhibition of ipsilateral BGMT, and thus allows ipsilateral thalamocortical activity to develop and cause contralateral movement initiation. The opposite is expected for unilateral activation of the SNr with ChR2, and was observed in our study, but only if SNr terminals were activated in BGMT. Direct unilateral activation of GABAergic SNr cell bodies resulted in strong bilateral movement inhibition instead (Fig. 3H). A recent set of studies have implicated the SNr nigrotectal pathway to the SC in the control of non-directional licking behavior

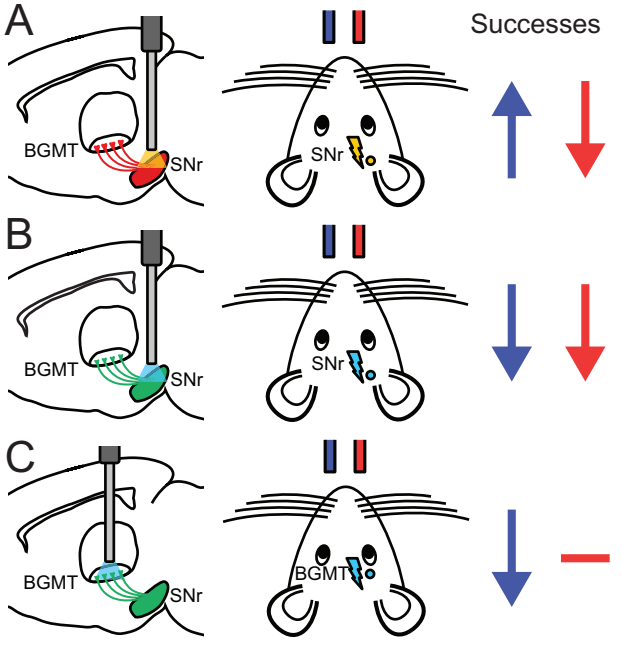

Fig. 5. Summary of optogenetic manipulations and main results. (A) Diagram depicting unilateral optogenetic inhibition of SNr expressing ARCH3 and orientation of lick spouts and mouse. SNr optogenetic inhibition is contralateral to the blue spout (left) and ipsilateral to the red spout (right). Optogenetic inhibition of the SNr produced a change in directional bias towards the contralateral spout (blue arrow) and away from the ipsilateral lick spout (red arrow). (B) Same as (A), but for experiments with unilateral optogenetic excitation of SNr expressing ChR2(ET/TC). Optogenetic excitation of the SNr produced a bilateral change in directional bias; decreasing licking activity towards both the contralateral (blue) and ipsilateral (red) lick spouts. (C) Same as (A) and (B), but for terminal excitation of SNr projections to the BGMT. Optogenetic excitation of SNr terminals in the BGMT produced a change in directional choice away from the contralateral spout (blue).

(Rossi et al., 2016; Toda et al., 2017). In Rossi et al. (2016), researchers used optogenetics to bilaterally excite SNr projections at the level of the SC, which led to diminished, though not completely suppressed, licking towards the lick spout positioned in front of the mouse. Our results showing that unilateral excitation of the SNr near completely suppressed licking could therefore be explained via projections to the SC. Consistent with this explanation, anatomical tracing experiments demonstrate that the SNr projects to SC bilaterally, while projections to the thalamus are ipsilateral (Deniau and Chevalier, 1992; Liu and Basso, 2008). Why somatic inhibition of the SNr did not facilitate licking bilaterally (opposite of SNr excitation) requires further examination but may suggest that the thalamic pathway is more susceptible to disinhibition than the nigro-SC pathway. It remains also possible that our SNr ChR2 expression was stronger than ARCH expression, and therefore might involve more cells than the ARCH inhibition. In addition, increases in SNr spike rate with ChR2 were 3.6-fold while inhibition was limited to decreasing the spike rate to zero. Such effects could explain a stronger effect exerted by ChR2 than by ARCH. However, the magnitude of contralateral behavioral effects was similar for ARCH and ChR2, and the statistically significant opposite effects of ARCH inhibition on ipsilateral and contralateral licking (Fig. 2H1) can also not be explained by differential opsin expression.

Our task did not require lick withholding during air-puff delivery and indeed we observed a steady increase in anticipatory licking activity as the start of the response period was approached. This licking was in the direction of the correct target, therefore revealing the completion of air-puff stimulus evaluation and motor preparation as early as 1 s before air-puff offset (Fig. 1C). Importantly, the prevalence of anticipatory licking was not affected by nigral ARCH activation (Fig. 2F), suggesting that tonic nigral inhibition in BGMT during reward anticipation was low when anticipatory licking was allowed, and therefore disinhibition had little effect on anticipatory licking. In contrast, a slowing of anticipatory licking was seen upon the onset of ChR activation of SNr terminals in BGMT for contralateral trials with a subsequent slowing of contralateral reward licks as well (Fig. 4C). This finding indicates that increased nigral inhibition of BGMT results in a lateralized slowing of movement. Several previous studies have shown that the BG exert lateralized control of motor circuits (Sakamoto and Hikosaka, 1989; Hikida et al., 2010; Tai et al., 2012; Dominguez-Vargas et al., 2017) and our results support this general concept. A slowing in licking is congruent with both the concepts of direct involvement of BG output in controlling movement velocity (Barter et al., 2015; Yttri and Dudman, 2016) or motor vigor (Dudman and Krakauer, 2016).

The BGMT with VM as its core component is well situated anatomically to influence ipsilateral cortical activity, with single-cell tracing studies in rodents depicting large projections branching across ipsilateral layer 1 of sensory and motor cortices (Kuramoto et al., 2009, 2015). BGMT in rodents is defined by strong inhibitory inputs from SNr (Kuramoto et al., 2011). We showed

here that optogenetic SNr manipulations could impact cortical decision-making processes about whisker stimulation dependent directional licking. Control of this behavior has previously been linked to a VM – ALM thalamocortical feedback loop (Li et al., 2015; Chen et al., 2017; Guo et al., 2017). The widespread axonal efferents of BGMT suggest that similar effects are likely for a multiplicity of other behaviors, and have in fact been demonstrated for locomotion (Roseberry et al., 2016) and head movement (Schmidt et al., 2013; Barter et al., 2015). To determine whether our manipulations inadvertently triggered such movements, we recorded high-speed video of the mouse pupil and face for a subset of trials across mice. Interestingly, we did not observe any movements (including eye, whisker, fore-limb) associated with our optogenetic manipulations (data not shown). Because it is unlikely that a uniform optogenetic inhibition or excitation across SNr codes for any specific behavioral event, it seems most likely that our optogenetic stimulation interfered with endogenous population coding, which in a highly trained mouse will be quite specific to the trained behavior. The detailed mechanism by which SNr mediated activity changes in BGMT impact cortical decision making remains unclear, especially since layer 1 is far removed from the activity of cell bodies in L5/6 providing output from cortex. A likely candidate mechanism for amplifying such distal input is given by active distal dendritic properties such as NMDA spikes in L2/3 (Palmer et al., 2014) and backpropagation activated Ca^{2+} spike firing in L5 pyramidal neurons (Larkum et al., 1999, 2001; Larkum and Zhu, 2002). Similar active properties are also seen in the apical dendrites of L6 pyramidal neurons (Ledergerber and Larkum, 2010), which have a strong projection back to BGMT (Yamawaki and Shepherd, 2015). In addition, BGMT input could also act on L1 interneurons (Cruikshank et al., 2012), which provide a powerful inhibition of pyramidal neuron dendrites (Palmer et al., 2012, 2013). The exact impact of BGMT input on these mechanisms and its integration into cortico-cortical information processing awaits future studies.

AUTHOR CONTRIBUTIONS

A.M., P.B., C.W., G.S., and D.J. designed research; A.M., P.C., and C.B. trained mice and performed optogenetic experiments; A.M. analyzed data; A.M. and D.J. wrote the paper.

ACKNOWLEDGEMENTS

This work was supported by the NIH/National Institute of Neurological Disorders and Stroke (NINDS) Brain Initiative Grant U01NS094302 (DJ & GS), T32 Training Grant 5T32HD071845 (AM), NIH F31 NRSA NS098691 (PB), and DFG Fellowship GZ: WA 3862/1-1 (CW).

REFERENCES

Aarts E, Verhage M, Veenvliet JV, Dolan CV, van der Sluis S (2014) A solution to dependency: using multilevel analysis to accommodate nested data. Nat Neurosci 17:491–496.

Albin RL, Young AB, Penney JB (1989) The functional anatomy of basal ganglia disorders. Trends Neurosci 12:366–375.

Alexander GE, Crutcher MD, DeLong MR (1990) Basal ganglia-thalamocortical circuits: parallel substrates for motor, oculomotor, "prefrontal" and "limbic" functions. Prog Brain Res 85:119–146.

Barter JW, Li S, Sukharnikova T, Rossi MA, Bartholomew RA, Yin HH (2015) Basal ganglia outputs map instantaneous position coordinates during behavior. J Neurosci 35:2703–2716.

Chen T-W, Li N, Daie K, Svoboda K (2017) A map of anticipatory activity in mouse motor cortex. Neuron 94:866–879.e864.

Cruikshank SJ, Ahmed OJ, Stevens TR, Patrick SL, Gonzalez AN, Elmaleh M, Connors BW (2012) Thalamic control of layer 1 circuits in prefrontal cortex. J Neurosci 32:17813–17823.

DeLong MR (1990) Primate models of movement disorders of basal ganglia origin. Trends Neurosci 13:281–285.

Deniau JM, Chevalier G (1985) Disinhibition as a basic process in the expression of striatal functions. II. The striato-nigral influence on thalamocortical cells of the ventromedial thalamic nucleus. Brain Res 334:227–233.

Deniau JM, Chevalier G (1992) The lamellar organization of the rat substantia nigra pars reticulata: distribution of projection neurons. Neuroscience 46:361–377.

Dominguez-Vargas AU, Schneider L, Wilke M, Kagan I (2017) Electrical microstimulation of the pulvinar biases saccade choices and reaction times in a time-dependent manner. J Neurosci 37:2234–2257.

Dudman JT, Krakauer JW (2016) The basal ganglia: from motor commands to the control of vigor. Curr Opin Neurobiol 37:158–166.

Efron B, Tibshirani RJ (1993) An Introduction to the Bootstrap. Chapman & Hall.

Freeze BS, Kravitz AV, Hammack N, Berke JD, Kreitzer AC (2013) Control of basal ganglia output by direct and indirect pathway projection neurons. J Neurosci 33:18531–18539.

Guo ZCV, Li N, Huber D, Ophir E, Gutnisky D, Ting JT, Feng GP, Svoboda K (2014a) Flow of cortical activity underlying a tactile decision in mice. Neuron 81:179–194.

Guo ZV, Hires SA, Li N, O'Connor DH, Komiyama T, Ophir E, Huber D, Bonardi C, Morandell K, Gutnisky D, Peron S, Xu N-L, Cox J, Svoboda K (2014b) Procedures for behavioral experiments in head-fixed mice. PLoS One 9 e88678.

Guo ZV, Inagaki HK, Daie K, Druckmann S, Gerfen CR, Svoboda K (2017) Maintenance of persistent activity in a frontal thalamocortical loop. Nature 545:181–186.

Hikida T, Kimura K, Wada N, Funabiki K, Nakanishi S (2010) Distinct roles of synaptic transmission in direct and indirect striatal pathways to reward and aversive behavior. Neuron 66:896–907.

Hikosaka O (2007) GABAergic output of the basal ganglia. Prog Brain Res 160:209–226.

Kuramoto E, Fujiyama F, Nakamura KC, Tanaka Y, Hioki H, Kaneko T (2011) Complementary distribution of glutamatergic cerebellar and GABAergic basal ganglia afferents to the rat motor thalamic nuclei. Eur J Neurosci 33:95–109.

Kuramoto E, Furuta T, Nakamura KC, Unzai T, Hioki H, Kaneko T (2009) Two types of thalamocortical projections from the motor thalamic nuclei of the rat: a single neuron-tracing study using viral vectors. Cereb Cortex 19:2065–2077.

Kuramoto E, Ohno S, Furuta T, Unzai T, Tanaka YR, Hioki H, Kaneko T (2015) Ventral medial nucleus neurons send thalamocortical afferents more widely and more preferentially to layer 1 than neurons of the ventral anterior-ventral lateral nuclear complex in the rat. Cereb Cortex 25:221–235.

Larkum ME, Zhu JJ (2002) Signaling of layer 1 and whisker-evoked Ca2+ and Na+ action potentials in distal and terminal dendrites of rat neocortical pyramidal neurons in vitro and in vivo. J Neurosci 22:6991–7005.

Larkum ME, Zhu JJ, Sakmann B (1999) A new cellular mechanism for coupling inputs arriving at different cortical layers. Nature 398:338–341.

Larkum ME, Zhu JJ, Sakmann B (2001) Dendritic mechanisms underlying the coupling of the dendritic with the axonal action

potential initiation zone of adult rat layer 5 pyramidal neurons. J Physiol 533:447–466.
Ledergerber D, Larkum ME (2010) Properties of layer 6 pyramidal neuron apical dendrites. J Neurosci 30:13031–13044.
Li N, Chen T-W, Guo ZV, Gerfen CR, Svoboda K (2015) A motor cortex circuit for motor planning and movement. Nature 519:51–56.
Li N, Daie K, Svoboda K, Druckmann S (2016) Robust neuronal dynamics in premotor cortex during motor planning. Nature 532:459–464.
Liu P, Basso MA (2008) Substantia nigra stimulation influences monkey superior colliculus neuronal activity bilaterally. J Neurophysiol 100:1098–1112.
Mink JW (1996) The basal ganglia: focused selection and inhibition of competing motor programs. Prog Neurobiol 50:381–425.
Oldenburg IA, Sabatini BL (2015) Antagonistic but not symmetric regulation of primary motor cortex by basal ganglia direct and indirect pathways. Neuron 86:1174–1181.
Palmer LM, Schulz JM, Larkum ME (2013) Layer-specific regulation of cortical neurons by interhemispheric inhibition. Commun Integr Biol:6.
Palmer LM, Schulz JM, Murphy SC, Ledergerber D, Murayama M, Larkum ME (2012) The cellular basis of GABAB-mediated interhemispheric inhibition. Science 335:989–993.
Palmer LM, Shai AS, Reeve JE, Anderson HL, Paulsen O, Larkum ME (2014) NMDA spikes enhance action potential generation during sensory input. Nat Neurosci 17:383–390.
Roseberry TK, Lee AM, Lalive AL, Wilbrecht L, Bonci A, Kreitzer AC (2016) Cell-type-specific control of brainstem locomotor circuits by basal ganglia. Cell 164:526–537.
Rossi MA, Li HE, Lu D, Kim IH, Bartholomew RA, Gaidis E, Barter JW, Kim N, Cai MT, Soderling SH, Yin HH (2016) A GABAergic nigrotectal pathway for coordination of drinking behavior. Nat Neurosci 19:742–748.
Sakamoto M, Hikosaka O (1989) Eye movements induced by microinjection of GABA agonist in the rat substantia nigra pars reticulata. Neurosci Res 6:216–233.
Schmidt R, Leventhal DK, Mallet N, Chen F, Berke JD (2013) Canceling actions involves a race between basal ganglia pathways. Nat Neurosci 16:1118–1124.
Svoboda K, Li N (2017) Neural mechanisms of movement planning: motor cortex and beyond. Curr Opin Neurobiol 49:33–41.
Tai LH, Lee AM, Benavidez N, Bonci A, Wilbrecht L (2012) Transient stimulation of distinct subpopulations of striatal neurons mimics changes in action value. Nat Neurosci 15:1281–1289.
Toda K, Lusk NA, Watson GDR, Kim N, Lu D, Li HE, Meck WH, Yin HH (2017) Nigrotectal stimulation stops interval timing in mice. Curr Biol 27:3763–3770.e3763.
van der Leeden R, Meijer E, Busing FMTA (2008) Resampling multilevel models. In: Handbook of Multilevel Analysis. New York, NY, US: Springer Science + Business Media. p. 401–433.
Yamawaki N, Shepherd GMG (2015) Synaptic circuit organization of motor corticothalamic neurons. J Neurosci 35:2293–2307.
Yttri EA, Dudman JT (2016) Opponent and bidirectional control of movement velocity in the basal ganglia. Nature 533:402–406.

(Received 24 April 2019, Accepted 17 October 2019)
(Available online 6 November 2019)